

EFFECTS OF THE STELLAR COMPONENT ON DERIVED PHYSICAL PARAMETERS OF GALACTIC H II REGIONS

Víctor Robledo-Rella¹

Instituto de Astronomía, Universidad Nacional Autónoma de México

RESUMEN

Presentamos resultados de espectroscopía espacialmente integrada de rendija larga en las regiones centrales de Carina, M8 y M20. Obtuimos dos tipos de espectros: *.neb* (nebuloso) y *.all* (nebuloso más estelar). Las abundancias *.neb* de (O/H) son menores ($\sim 0.10 - 0.30$ dex) respecto del caso *.all*.

ABSTRACT

We present results of long-slit spatially integrated (~ 7 arcmin 2) spectroscopy (3600 – 10200 Å) in the central regions of Carina, M8 and M20. We obtained two types of spectra: *.neb* (pure nebular) and *.all* (nebular plus stellar). The stellar effect increases along the Balmer series, with *.neb/.all* ~ 1.20 at H δ , but could be much stronger (~ 1.7) for weaker lines beyond H8. The resulting *.neb* dereddened spectra give slightly higher electron temperatures which yield (O/H) smaller ($\sim 0.10 - 0.30$ dex), (N/H) higher ($\sim 0.05 - 0.10$ dex), (Ne/H) smaller ($\sim 0.25 - 0.40$ dex), and (Ar/H) smaller ($\sim 0.15 - 0.30$ dex), with respect to the *.all* case. Although these differences are roughly within the uncertainties, they could be important in deriving accurate chemical compositions in extragalactic nebula where the stars are not resolved.

Key Words: ABUNDANCES — H II REGIONS — ISM: INDIVIDUAL (CARINA, M8, M20)

The results presented here are part of a study aimed at estimating quantitatively the effect of the exciting stars' spectra on the observed nebular spectra for a set of selected galactic H II regions. The main motivation for this work comes from studies of extragalactic H II regions (and H II galaxies) in which this underlying stellar contribution is only roughly approximated.

The observations were carried out with the 1.5-m Telescope at CTIO, using a Cassegrain spectrograph, with an average resolution of ~ 12 Å FWHM over the spectral range 3600 – 10200 Å. We aligned N–S a 7.5 arcmin long slit and adjusted the tracking rate of the telescope so as to scan a square area (~ 7 arcmin 2) on the center of Carina, M8 and M20. The selection of the whole sample was made on the basis of knowing *a priori* the spectral type (SpT) and luminosity class (LC) of the stars (presumably) responsible for the ionization. The Carina Nebula was divided in 3 subregions: CarNW, CarSE (which includes η Car) and CarSW. M8 and M20 were divided in 2 subregions each: M8–E, M8–W, M20–S and M20–N. The SpT and LC of the bright (and hot) stars identified in each subregion are given in Table 1.

The data were reduced using standard procedures within IRAF, with special attention paid to the illumination-correction process. We extracted the spectra (along the spatial direction) in two different ways: *.all* case, in which we included both the nebular spectra as well as the stars' spectra passing over the slit during the scans, and, *.neb* case, in which we “removed” the stars' spectra before the extraction. We removed all stars with a continuum at $\lambda 4861 \geq 5\%$ of the H β nebular emission (Table 1). We estimate our flux-calibration is accurate within $\sim 5 - 8\%$. Dark-sky subtraction introduces an extra $\sim 10\%$ uncertainty for $\lambda \geq 7000$ Å. In Figure 1 we plot for each subregion the parameter $r \equiv [F(\lambda).neb/F(\lambda).all]_{obs}$ as function of λ for the Balmer lines.

We derived (*.all* and *.neb*) extinction laws for Carina applying a 5th-order polynomial fit to the ratios $[F_\lambda/F_{H\beta}]_{obs}/[F_\lambda/F_{H\beta}]_{theo}$ as a function of λ^{-1} for the Balmer and Paschen lines, and found a logarithmic

¹Based on observations from CTIO, a division of NOAO, which is operated by AURA, Inc. under agreement with NSF.

TABLE 1
SPECTRAL TYPES OF EXCITING STARS

CarNW	CarSE	CarSW	M8-E	M8-W	M20-S & M20-N
O3 V ((f))	LBV (η Car)	O3-O4 If	O4 V ((f))	O7.5 V(n)	O7.5 III ((f))
O3 If*	O3 V ((f))	WN7+abs	O6.5 V ^a	K4 III?	B6 V
O6 V ((f))	O3 V	B0 V	O9.5 IVn ^a		A2 Ia
O6 III (f)	O5 V ((f))	B1 V	B2.5 V		A5 Ia ^a
O6.5 V ((f))	O6 V ((f))	B1 V	B3 Ve		F3 V
O8 V	O7 V ((f))	B1.5 V	B5.5 V		
O9 V	O8 V	B1.5 V	K0 III		
B0 III-IV	O8.5 V				
B0.5 IV-V					
B1 V					

^a These stars are not within our subregions: the O9.5 IVn is $\sim 0.7'$, the O6.5 V is $\sim 13.4'$, and the A5 Ia is $\sim 1'$, away from our subregion edges.

reddening correction factor, $c(H\beta) = 1.00 \pm 0.5$, a total visual extinction, $A_V = 2.3 \pm 0.3$ mag, and a ratio of total to selective extinction, $R = A_V/E_{B-V} = 4.4 \pm 0.4$, in reasonable agreement with other authors (e.g., Tapia et al. 1988). M8 and M20 spectra were dereddened applying 4 values of $c(H\beta)$ (from different Balmer and Paschen line ratios) to selected λ intervals, assuming a Cardelli, Clayton, & Mathis (1989) extinction law, $f(\lambda)$, with $R = 3.1$. We found $c(H\beta) = 0.6-0.7$ and $0.6-0.9$, for M8 and M20, respectively.

We then computed intrinsic (.all and .neb) line fluxes for each subregion, needed to derive their physical conditions. We computed electron densities, N_e , electron temperatures, T_e , and ionic abundances (relative to H⁺) of O⁺(3727), O⁺⁺(5007), N⁺(6584), S⁺(6725), S⁺⁺(9531), Ne⁺⁺(3869), and Ar⁺⁺(7136) using a set of ionic-emissivities (*Abelion*), $\epsilon(X_\lambda^{+m}, T_e)$, courtesy of G. Stasińska. We derived total abundances (relative to H) for O, N, S, Ne, and Ar using the ionization correction factors (ICFs) of Kingsburgh & Barlow (1994).

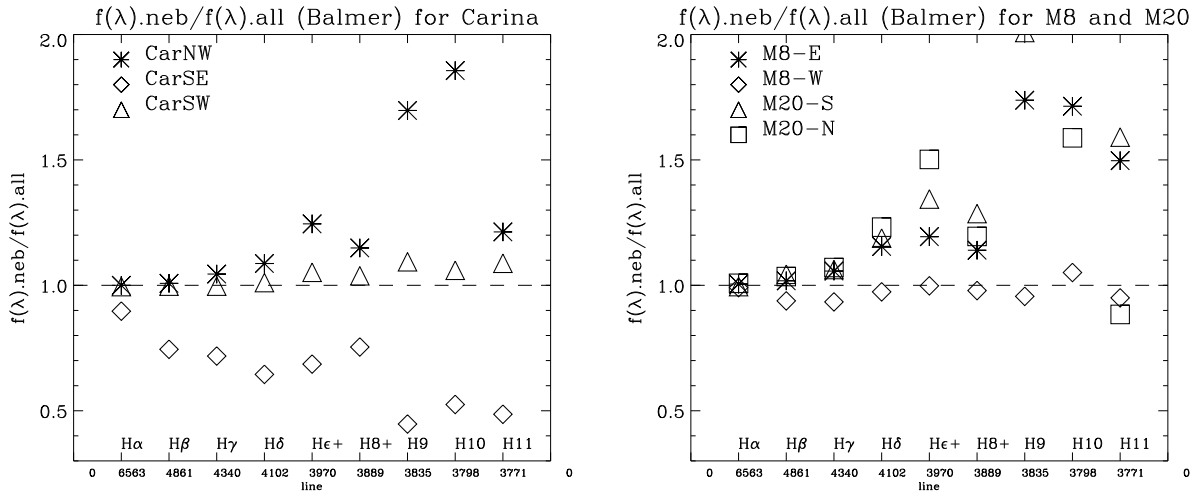


Fig. 1. Balmer lines $F(\lambda).neb/F(\lambda).all$ parameter for Carina (left) and M8 and M20 (right) subregions.

Physical parameters (.all and .neb) for the Carina subregions have been given in Robledo-Rella & Peña (1999). For M8-E and M8-W we found the following .neb average values: $N_e = 300 \pm 70\% \text{ cm}^{-3}$, $T_{\text{OIII}} =$

TABLE 2
COMPARISON OF PHYSICAL PARAMETERS

ID	CarNW	CarSE	CarSW	M8-E	M8-W	M20-S	M20-N	error
N_{SII}	1.00	1.50	0.75	1.19	0.97	1.00	1.20	$\pm 70\%$
T_{OIII}	1.05	—	1.03	1.02	1.07	0.92	0.98	$\pm 7\%$
T_{NII}	1.01	1.60	1.13	1.05	1.00	1.02	0.98	$\pm 11\%$
$\text{O}^+(3727)$	-0.16	+0.62	+0.05	-0.32	-0.05	-0.32	-0.13	± 0.12
$\text{O}^{++}(5007)$	+0.06	+0.17	+0.11	-0.03	-0.15	+0.10	+0.02	± 0.10
$\text{N}^+(6584)$	+0.01	+0.09	+0.03	-0.06	-0.04	+0.01	+0.02	± 0.10
$\text{S}^+(6725)$	+0.02	+0.21	+0.02	-0.05	-0.03	+0.02	+0.02	± 0.10
$\text{S}^{++}(9531)$	-0.01	+0.20	-0.04	-0.05	-0.05	-0.01	+0.02	± 0.08
$\text{Ne}^{++}(3869)$	-0.05	+0.22	+0.09	-0.10	-0.18	-0.06	-0.17	± 0.12
$\text{Ar}^{++}(7136)$	+0.04	+0.04	+0.06	-0.03	-0.09	+0.07	+0.02	± 0.10
O/H	-0.07	+0.28	+0.09	-0.16	-0.09	-0.30	-0.13	± 0.12
N/H	+0.11	-0.26	+0.06	+0.10	-0.08	+0.03	+0.02	± 0.15
S/H	+0.00	+0.12	-0.03	-0.03	-0.06	+0.00	+0.02	± 0.15
Ne/H	-0.19	+0.33	+0.09	-0.23	-0.12	-0.46	-0.32	± 0.18
Ar/H	-0.09	+0.15	+0.04	-0.16	-0.03	-0.33	-0.13	± 0.15
ICF(N)	1.25	0.45	1.09	1.44	0.90	1.04	1.01	$\pm 11\%$
ICF(S)	1.02	0.82	1.02	1.06	0.99	1.00	1.00	$\pm 5\%$
ICF(Ne)	0.75	1.27	0.96	0.74	1.13	0.39	0.70	$\pm 8\%$

N_e , T_e and ICFs give ratio $.neb/.all$ (linear). Ionic and total abundances give difference $.neb - .all$ (dex). The errors correspond to the given parameter.

$7.6 \pm 7\%$ kK, $T_{\text{NII}} = 8.4 \pm 11\%$ kK, O = 8.64 ± 0.12 , N = 7.58 ± 0.15 , S = 6.78 ± 0.15 , Ne = 7.87 ± 0.15 and Ar = 6.58 ± 0.15 . Similarly, for M20-S and M20-N we found: $N_e = 80 \pm 70\% \text{ cm}^{-3}$, $T_{\text{OIII}} < 11.0 \pm 10\%$ kK, $T_{\text{NII}} = 8.8 \pm 11\%$ kK, O = 8.48 ± 0.12 , N = 7.32 ± 0.15 , S = 6.67 ± 0.15 , Ne = 7.43 ± 0.15 and Ar = 7.06 ± 0.15 . The comparison of $.neb$ vs. $.all$ physical parameters for each subregion is given in Table 2.

REFERENCES

- Cardelli, J. A., Clayton, G. C., & Mathis, J. S. 1989, ApJ, 345, 245
- Kingsburgh, R. L., & Barlow, M. J. 1994, MNRAS, 271, 257
- Robledo-Rella, V., & Peña, M. 1999, in IAU Symp. 193, Wolf-Rayet Phenomena in Massive Stars and Starburst Galaxies, ed. K. A. van der Hucht, G. Koenigsberger, & P. R. J. Eenens (San Francisco: ASP), 493
- Tapia, M., Roth, M., Marraco, H., & Ruiz, M. T. 1988, MNRAS, 32, 661